UDC 629.5.052.3+621.396.67.012.12

ACCURATE DETECTION OF MULTIPLE TARGETS BY UNIFORM RECTANGULAR ARRAY RADAR WITH THRESHOLD SOFT UPDATE AND AREA RESCANNING

Vadim V. Romanuke

Polish Naval Academy, Gdynia, Poland

Background. If the intensity of moving targets within a surveyed area is low, an optimal number of uniform rectangular array (URA) radar sensors is in either the minimally-sized URA (or close to it) or maximally-sized URA (or close to it), where the URA size is regulated by (symmetrically) turning off vertical and horizontal sensors. However, this does not guarantee detection of any target because sometimes the threshold detection, by which the main parameters of a pair of two targets are estimated, fails even by using the soft threshold approach when the threshold is gradually decreased while the detection fails.

Objective. In order to improve detection of multiple ground-surface targets by a URA radar, the goal is to decrease a number of detection fails, when targets are just missed. For this, the approach of threshold soft update and a set of quasioptimal URA sizes included 20×25 and 35×35 URAs are to be used by rescanning the area if the detection fails.

Methods. To achieve the goal, the functioning of the URA radar is simulated for a set of randomly generated targets, where roughly a half of the set is to be of single targets, and the other half is to be of pairs of targets. The simulation is configured and carried out by using MATLAB® R2021b Phased Array System Toolbox™ functions based on a model of the monostatic radar.

Results. Neither the soft threshold approach, nor the rescanning increase the detection accuracy. However, when either the soft threshold or rescanning is applied, or they both are applied, the number of detections is increased. The increment can be evaluated in about 2.7 %, but the expected high-accurate detection performance slightly drops. This is caused by that the soft thresholding and rescanning attempt at retrieving at least some information about the target instead of the detection fail.

Conclusions. Using the threshold soft update approach along with a more frequent rescanning decreases a number of detection fails. Besides, the soft thresholding and rescanning allow slightly decreasing the number of URA sensors sufficient to maintain the same detection accuracy by increasing the averaged number of single-target and two-target detections at least by 2.5 %. The increment in a number of detected targets on average is equivalent to increasing the probability of detection.

Keywords: *phased array radar; uniform rectangular array; surveyed area; target; detection threshold; rescanning.*

1. Phased array radar issues

A uniform rectangular array (URA) radar can be used to observe and control presence of multiple ground-surface objects (sometimes also called targets) within a nearby area [1], [2]. The URA radar is a static mechanic system that scans the area without turning the antenna elements (URA sensors) [2], [3]. This is done by using the phase shifters [4], [5] delaying the radio waves progressively so that each sensor emits its wavefront in a specific order. This causes the resulting plane wave to be directed at a required angle to the URA. The computer quickly alters the phase shifters to steer the beam of radio waves to a new direction, which usually is in the neighborhood of the previous direction [6], [7].

The scanning range S of azimuth angles can be up to 90° and wider, and the area is scanned through a scan grid. The scan grid is a set

$$G_{\text{scan}}=\left\{\vartheta_i\right\}_{i=1}^{K} \tag{1}$$

of azimuth angles in degrees. Grid (1) is usually formed to be uniform and symmetric with a scanning step of δ_{scan}. It starts with

$$\vartheta_1=\frac{S}{2}-\frac{S-\rho\left(S/\delta_{\text{scan}}\right)\cdot\delta_{\text{scan}}}{2}=\rho\left(\frac{S}{\delta_{\text{scan}}}\right)\cdot\frac{\delta_{\text{scan}}}{2}, \tag{2}$$

where function $\rho(\theta)$ returns the integer part of number θ (e. g., see [8], [9]), and goes down with a step of $-\delta_{\text{scan}}$ until $\vartheta_K\geqslant -S/2$:

$$\vartheta_{i+1}=\vartheta_i-\delta_{\text{scan}} \text{ for } i=\overline{1,\,K-1}. \tag{3}$$

The scanning schedule of the URA must be sufficiently tight. The radar should revisit the same azimuth angle within at most 1 second. The required number of scans is determined by the beamwidth of the array response. The 3 dB beamwidth θ (in degrees) is estimated by using the array gain. Then the scanning step δ_{scan} is selected so that $\delta_{\text{scan}}<\theta$ to have some beam overlap in space. To hold a sufficiently dense scan grid, the scanning step must not be greater than $6°$. So, the scanning step is

$$\delta_{\text{scan}}=\min\left\{6,\,\rho(\theta)\right\}. \tag{4}$$

Except for a narrow "pencil" beam mainlobe, no specific beam pattern, for ensuring signal selectivity by direction, is synthesized for the URA radar [10], [11]. The beam pattern mainlobe for the URA radar must be symmetric and sufficiently narrow at any scanning direction [4], [12], [13]. To maintain low interference, the beam sidelobes must be cancelled at both the azimuth and elevation angles (Fig. 1).

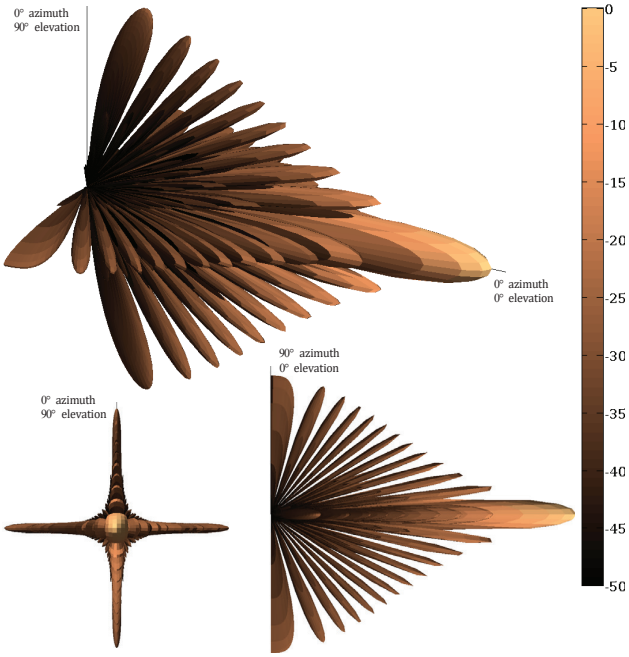

Fig. 1. A 20×25 URA response pattern (the colorbar is normalized power in dB, so lighter color corresponds to greater power emitted) [14]

Although the ground-surface URA radar does not observe or control presence at (positive) elevation angles, the power emitted at elevations should be as little as possible. This is why URA vertical sensors are used in such radars. For instance, the number of vertical sensors of the URA in Fig. 1 is less than the number of horizontal sensors, but still those 20 sensors ensure small losses of power at elevations and additionally form the narrow "pencil" beam mainlobe. So, a radar of URA with only 5 vertical sensors would be quite inefficient (Fig. 2). Moreover, it was ascertained in [14] that, in detecting a single target, the 20×25 URA radar has roughly the best performance (see Fig. 11 in [14]). The performance is evaluated by using relative differences (in percentage terms)

$$\Delta_d = 100\cdot\frac{|d^*-d|}{d}, \tag{5}$$

$$\Delta_\alpha = 100\cdot\frac{|\alpha^*-\alpha|}{90} = \frac{|\alpha^*-\alpha|}{0.9}, \tag{6}$$

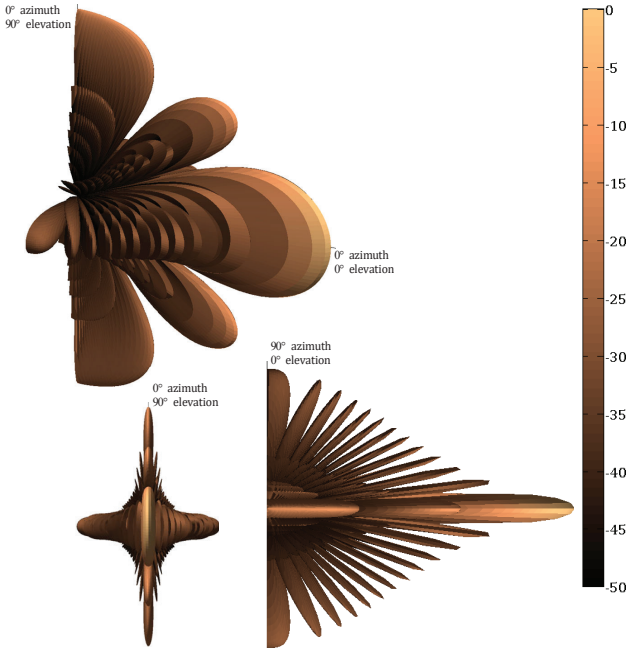

Fig. 2. A 5×25 URA response pattern, where the ineffectiveness of the 5×25 URA radar is seen (compared to that in Fig. 1) due to much power is emitted at elevations and the beam mainlobe is not sufficiently narrow at the side elevation view (although it is quite narrow at the pattern view from "above" being similar to that in Fig. 1) [14]

and

$$\Delta_v = 100\cdot\left|\frac{v^*-v}{v}\right| \tag{7}$$

for the main parameters of a target — distance d to the target (in terms of radar systems, it is also called the range), azimuth angle α, and velocity v, where d^*, α^*, and v^* are the respective estimations of these parameters.

It was also ascertained in [14] that an optimal number of URA radar sensors is in either the minimally-sized URA (or close to it) or maximally-sized URA (or close to it), where the URA size is regulated by (symmetrically) turning off vertical and horizontal sensors. The set of those quasioptimal URA sizes is

$$\begin{aligned} &20\times25,\ 35\times35,\ 20\times26,\ 34\times35,\\ &20\times27,\ 33\times35,\ 20\times28,\ 34\times34,\\ &20\times29,\ 33\times34,\ 20\times30,\ 33\times33. \end{aligned} \tag{8}$$

Besides, the threshold detection stage was modified in [14] so that the threshold was gradually (softly) decreased while the detection failed. This approach allows increasing a number of singly detected targets on average, but will it perform similarly when two targets

are simultaneously present within the radar area? The matter is that even when a URA radar works for detecting a single target, the likelihood of missing a target is not that small. For instance, 12 of 500 targets simulated in [14] were not detected by using the threshold soft update approach (see Fig. 11 in [14]).

2. Goal and tasks to achieve it

To improve detection of multiple ground-surface targets, the goal is to decrease a number of detection fails, when targets are just missed. For this, the approach of threshold soft update and set (8) of quasioptimal URA sizes will be used. To achieve the said goal, the URA radar is to be simulated by using MATLAB® R2021b Phased Array System Toolbox™ (PAST) functions. First, the simulation parameters and set-up are to be described. Next, the functioning of the URA radar is simulated for a set of randomly generated targets, where roughly a half of the set is to be of single targets, and the other half is to be of pairs of two targets. A target or a pair of two targets is tried to be detected by 20×25 URA. If the detections fails, the URA size is set at 35×35. While the detections fails, the URA size is further tried at

$$20\times 26,\ 34\times 35,\ ...,\ 20\times 30,\ 33\times 33,$$

according to the ascending list in set (8), where changing the URA size is meant by turning on or off some sensors. The simulation will be carried out for both the known (hard) threshold detection approach and the threshold soft update approach (softer adjustment approach), by rescanning the area if the detection fails and without rescanning. The results obtained from the simulation are expected to increase the detection probability without affecting the accuracy of estimation of the target parameters. All limitations, tradeoffs, and controversies of the threshold soft update and area rescanning approach will be discussed.

3. Simulation parameters

It is supposed that a URA is used in a monostatic radar to periodically scan a predefined surveillance area [4], [15]. The purpose is to detect either a target or two targets in this region and estimate their main parameters $\{d, \alpha, v\}$. Targets are only sought in the azimuth dimension, and the radar is required to search from $45°$ to $-45°$ in azimuth, where scan grid (1) starts with

$$\vartheta_1 = \rho\left(\frac{90}{\delta_{\text{scan}}}\right)\cdot\frac{\delta_{\text{scan}}}{2} \tag{9}$$

and goes down with a step of $-\delta_{\text{scan}}$ until $\vartheta_K \geqslant -45°$:

$$\vartheta_{i+1} = \vartheta_i - \delta_{\text{scan}} \text{ for } i = \overline{1,\ K-1}. \tag{10}$$

The URA radar created by using the PAST environment and functions is designed by the typical specifications: detection probability is $p_{\text{det}} = 0.9$, probability of false alarm is $p_{\text{FA}} = 10^{-6}$, maximum unambiguous range is $r_{\max} = 5000$ (in meters), target radar cross section is $1\ \text{m}^2$, the number of pulses to integrate is 10. The parameters of the URA radar are as follows:

1) the operating frequency $f_{\text{oper}} = 10$ GHz;

2) the sampling frequency $f_{\text{sampl}} = 5995849.16$ Hz;

3) the pulse repetition frequency (f_{PR}) is presumed to be a $1/200$ part of the sampling frequency, so it is $f_{\text{PR}} = 29979.2458$ Hz.

The URA consists of w horizontal and h vertical antenna elements emitting only forward. The array gain, signal-to-noise ratio, and the peak power are calculated using radar equations [4], [12], [13], [16], [17]. Then the peak power of the transmitter is set [14].

The total number of pulses is $10\cdot K$, so the revisit time is

$$t_{\text{rev}} = \frac{10\cdot K}{f_{\text{PR}}} = \frac{10\cdot K}{29979.2458} \approx$$
$$\approx 0.0003335640952\cdot K. \tag{11}$$

As the URA is grown in size, the revisit time increases due to the scan grid becomes denser (and thus number K increases). However, even for relatively huge URAs (of 100×100 size and bigger) revisit time (11) is far less than 1 second [18], [19].

Either a single target or a pair of two targets is assumed to be at $0°$ elevation. Besides, neither target is a fluctuating object [20], [21]. Pulses emitted by the URA, propagation channels, and reflected signals received by the URA are simulated by the PAST environment. So, a pulse is generated, emitted, radiated toward the target, and reflected off the target. This is repeated for $10\cdot K$ pulses. Then the received signal is processed by passing it through a matched filter and integrating all pulses for each scan angle [22], [23].

To estimate each target parameters $\{d, \alpha, v\}$, a threshold detection on the scan map is fulfilled. The detection threshold γ is firstly calculated based on the number of pulses to be integrated and noise power at the receiver. Then, however, the threshold is increased by the matched filter processing gain.

4. How the detection may fail

The pulse integration at the stage of threshold detection is fulfilled by compensating for signal power loss due to range by applying time varying gains to the

received signal. The result of the pulse integration is a matrix

$$\mathbf{Q}=\left[q_{ji}\right]_{200\times K}$$

whose elements are very small (roughly between 10^{-20} and 10^{-6}). Then inequality

$$q_{ji}^2>\gamma \tag{12}$$

is analyzed to estimate the range and angle of each target. Those indices j and i for which inequality (12) holds (denote them by j^* and i^*) point to the estimated range (distance to the target) and azimuth angle, respectively. This is done by mapping index j^* on a grid of ranges

$$G_{\text{range}}=\left\{r_j\right\}_{j=1}^{200}=\left\{25\cdot\left(j-1\right)\right\}_{j=1}^{200},$$

whereas index i^* is mapped on the scan grid G_{scan}. Thus, the estimated range d^* and azimuth angle α^* are determined. If inequality (12) does not hold, indices j^* and i^* are not found, and then the detection is counted as a fail [14].

The radial velocity (in meters per second) v^* of the target is calculated based on the Doppler shift [24], [25], where matched filtering pulses, indices j^*, i^*, and pulse repetition frequency f_{PR} are used. First, the Doppler spectrum from the received signal is calculated [13], [26], [27]. Second, its peak points to the respective velocity estimation. However, if the peak is impossible to find, the detection is counted as a fail [14].

5. How the target parameters are generated

The location of a target is given as a pair of its coordinates

$$\left\{x,y\right\}\ \text{by}\ x>0\ \text{and}\ y\in\mathbb{R}. \tag{13}$$

The distance to the target is

$$d=\sqrt{x^2+y^2} \tag{14}$$

and its azimuth angle is

$$\alpha=\frac{180}{\pi}\cdot\arctan\left(\frac{y}{x}\right). \tag{15}$$

Coordinates (13) of every simulated target are randomly generated as

$$x=\rho\left(4950\xi+50\right) \tag{16}$$

and

$$y=\rho\left(4950\zeta_1+50\right), \tag{17}$$

where ξ is a value of a random variable uniformly distributed on interval $(0;1)$ and ζ_1 is a value of a random variable distributed normally with zero mean and unit variance [14]. If coordinates (16) and (17) are such that $d>4975$ or $\alpha>44°$, their generations by (16) and (17) are repeated until $d\leqslant 4975$ and $\alpha\leqslant 44°$.

The velocity of a target is given in two coordinates:

$$\left\{v_x,v_y\right\}\ \text{by}\ v_x\in\mathbb{R}\ \text{and}\ v_y\in\mathbb{R}. \tag{18}$$

Velocity coordinates (18) are randomly generated as

$$v_x=\rho\left(100\zeta_2\right) \tag{19}$$

and

$$v_y=\rho\left(100\zeta_3\right), \tag{20}$$

where ζ_2 and ζ_3 are values of independent random variables distributed normally with zero mean and unit variance. The radial velocity of the target is calculated as [28], [29]

$$v=-\frac{xv_x+yv_y}{d} \tag{21}$$

(in meters per second).

6. The volume of radar simulations

The factual size of the URA is 35×35, where a URA of any other size below 35×35 is obtained by turning off the respective number of sensors [30], [31]. The turned-off sensors are expected to be in some symmetry with respect to the URA geometry. It is presumed that the symmetry of the sensors to be turned off is calculated and implemented automatically by a special computer routine [32]. As either a new single target or a pair of two targets is generated by equations (16), (17), (19), (20), the URA size is set according to the ascending list in (8).

If $\xi_0>0.5$, where ξ_0 is a value of a random variable uniformly distributed on interval $(0;1)$, then a pair of two targets (an instance) is generated; otherwise — a single target (an instance) is generated. For obtaining statistically stable results, it is sufficient to simulate 5000 random instances.

7. Threshold soft update and area rescanning

The detection straightforwardly fails if inequality (12) does not hold. So, while

$$q_{ji}^2\leqslant\gamma \tag{22}$$

the threshold is updated so that it would fit inequality (12):

$$\gamma^{(\text{obs})} = \gamma\,,\ \gamma = \left(\gamma^{(\text{obs})}\right)^{1.0001}, \tag{23}$$

whereupon inequality (12) is checked again. If inequality (12) is false and $\gamma < 10^{-50}$, the threshold updating is cancelled and thus the detection is counted as a fail [14].

If the detection fails, the area is rescanned. As the target continues moving, its coordinates (13) are updated according to velocity coordinates (18):

$$x^{(\text{obs})} = x\,,\ x = x^{(\text{obs})} + 0.2kv_x\,, \tag{24}$$

$$y^{(\text{obs})} = y\,,\ y = y^{(\text{obs})} + 0.2kv_y\,, \tag{25}$$

where k is the rescanning number, $k = \overline{1, 5}$. Having the rescanning switched off is conditional as it means that its frequency is low, and the target may move aside so that it is hard to identify whether it is the same ("old") target or not.

8. Results

The results of simulating 5000 random instances with (16), (17), (19), (20), and (24), (25) can be processed and presented in the following nine subcases (for the known or hard threshold detection approach and the threshold soft update approach):

1. Number of single-target detections when the rescanning has been either not applied or switched off.
2. Number of two-target detections when the rescanning has been either not applied or switched off.
3. Number of single-target detections when the rescanning has been applied.
4. Number of two-target detections when the rescanning has been applied.
5. Total number of detections when the rescanning has been either not applied or switched off.
6. Total number of detections when the rescanning has been applied.
7. Total number of single-target detections.
8. Total number of two-target detections.
9. Total number of detections.

An important factor is relative difference maximum

$$m_\Delta = \max\{\Delta_d, \Delta_\alpha, \Delta_v\} \tag{26}$$

compared to an acceptable (tolerable) percentage of inaccuracy a_{est} in the estimations of the target parameters [14]. The results of comparisons to various a_{est} (including intolerable ones) are presented in Table 1 (according to the above-listed numeration). It is seen that, in general, the greater percentage of relatively accurate detections has been obtained for the soft threshold and rescanning (highlighted bold). The exception is the cases for $m_\Delta < 2$, where only the soft threshold detection has a lesser percentage. This is explained with that, for a given URA size, the rescanning is applied every time when the detection fails. If the rescanning fails itself, the URA size is changed according to the ascending list in (8). Thus, there are 320 detections out of 5000, where relative difference maximum (26) is lesser for the hard threshold. However, the soft threshold has used 24 URAs of sizes 20×25 and 35×35 for 296 times, respectively, whereas the hard threshold has used

$$20\times25\,,\ 20\times26\,,\ 20\times27\,,\ 20\times28\,,\ 20\times29\,,\ 20\times30\,,\ 34\times34\,,\ 35\times35$$

sizes for 167, 3, 8, 1, 1, 1, 3, 136 times, respectively.

Table 1. Percentage of detections (instances) for relative difference maximum (26)

$m_\Delta < a_{\text{est}}$	Threshold	Percentage of detections (instances)								
		1	2	**3**	**4**	5	**6**	7	8	9
$m_\Delta < 1$	hard	**4.04**	**0.28**	**5.48**	**0.36**	**4.32**	**5.84**	**9.52**	**0.64**	**10.16**
	soft	3.98	0.22	5.34	0.26	4.2	5.6	9.32	0.48	9.8
$m_\Delta < 1.5$	hard	**9.9**	**1.66**	**11.36**	**1.94**	**11.56**	**13.3**	**21.26**	**3.6**	**24.86**
	soft	9.74	1.28	11	1.58	11.02	12.58	20.74	2.86	23.6
$m_\Delta < 2$	hard	**15.3**	**3.64**	**18.14**	**4.5**	**18.94**	**22.64**	**33.44**	**8.14**	**41.58**
	soft	15.04	3.22	17.38	3.8	18.26	21.18	32.42	7.02	39.44
$m_\Delta < 3$	hard	18.3	5.1	**22.5**	6.7	23.4	**29.2**	**40.8**	11.8	52.6
	soft	**18.58**	**6.98**	21.08	**7.22**	**25.56**	28.3	39.66	**14.2**	**53.86**
$m_\Delta < 4$	hard	18.88	5.52	**23.1**	7.8	24.4	30.9	**41.98**	13.32	55.3
	soft	**19.94**	**9.54**	21.72	**9.24**	**29.48**	**30.96**	41.66	**18.78**	**60.44**
$m_\Delta < 5$	hard	19.44	5.62	**23.56**	8.38	25.06	31.94	**43**	14	57
	soft	**20.7**	**9.88**	22.2	**9.98**	**30.58**	**32.18**	42.9	**19.86**	**62.76**
$m_\Delta < 7$	hard	19.9	5.9	**24.12**	9.08	25.8	33.2	44.02	14.98	59
	soft	**21.24**	**10.36**	22.82	**10.88**	**31.6**	**33.7**	**44.06**	**21.24**	**65.3**
$m_\Delta < 10$	hard	20.24	6.1	**24.64**	9.82	26.34	34.46	44.88	15.92	60.8
	soft	**22.28**	**10.86**	23.46	**11.68**	**33.14**	**35.14**	**45.74**	**22.54**	**68.28**
$m_\Delta < 15$	hard	20.44	6.36	**24.86**	10.28	26.8	35.14	45.3	16.64	61.94
	soft	**22.76**	**11.22**	23.86	**12.22**	**33.98**	**36.08**	**46.62**	**23.44**	**70.06**
$m_\Delta < 20$	hard	20.64	6.48	**25.06**	10.8	27.12	35.86	45.7	17.28	62.98
	soft	**23**	**11.46**	24.06	**12.7**	**34.46**	**36.76**	**47.06**	**24.16**	**71.22**
$m_\Delta < 25$	hard	20.72	6.66	**25.08**	11.02	27.38	36.1	45.8	17.68	63.48
	soft	**23.1**	**11.66**	24.08	**12.98**	**34.76**	**37.06**	**47.18**	**24.64**	**71.82**
$m_\Delta < 50$	hard	20.96	7.56	**25.18**	12.64	28.52	37.82	46.14	20.2	66.34
	soft	**23.34**	**12.48**	24.14	**14.22**	**35.82**	**38.36**	**47.48**	**26.7**	**74.18**

In grand total, the hard threshold has detected 4789 instances (2373 single-target detections and 2416 two-target detections), which is 95.78 %. The soft threshold has detected 4921 instances (2443 single-target detections and 2478 two-target detections), which is 98.42 %. The overall effect of the rescanning along with the soft threshold approach can be evaluated from Table 2.

Table 2. Percentage of detections (instances) for relative difference maximum (26)

Threshold detection	Number of detections		Percentage	
	No rescanning	Rescanning	No rescanning	Rescanning
hard	2021	**2768**	0.4042	**0.5536**
soft	**2347**	2574	**0.4694**	0.5148

The scatter of targets which have been missed is presented in Fig. 3. There are 130 single-target and 81 two-target omissions made by the hard threshold radar, whereas the soft threshold radar has omitted 60 single-target and 19 two-target detections. In fact, the subplot for the soft threshold radar (on the right) shows the impact of applying the soft thresholding to significantly reduce fails (omissions) of detection. Although it does not increase the accuracy of the estimated parameters, the reveal of that there is (at least somewhere within the observed area) a presence is itself very valuable information. Unfortunately, it is not seen any pattern in Fig. 3 which could help in forecasting subareas where reliable detection is less probable. It appears that the detection fail can appear in any point of the area.

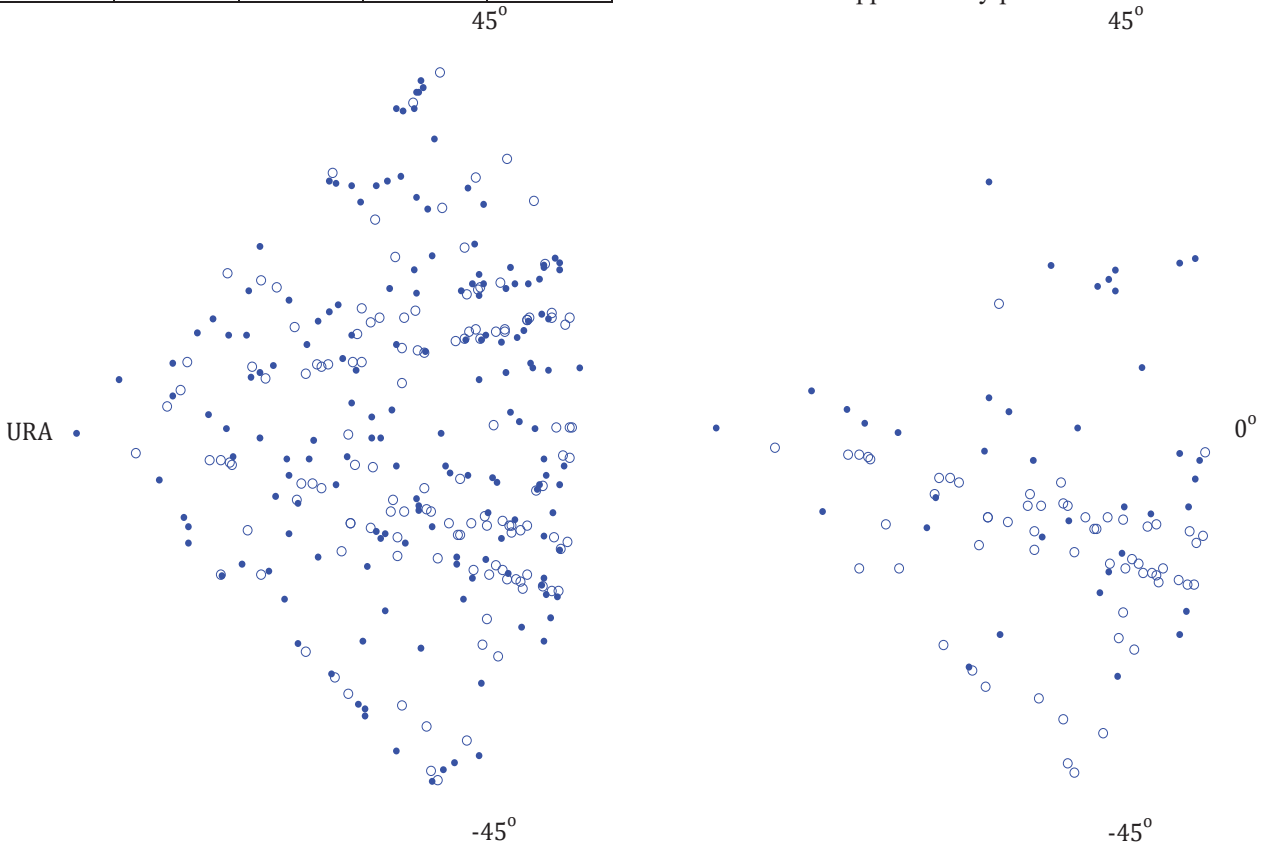

Fig. 3. The single-target omissions (circles) and two-target omissions (each target is a dot) by the hard threshold radar (left) and soft threshold radar (right)

As the velocity increases, it is more difficult to "catch" the target. However, if a target is moving too fast, the rescanning has its favorable impact. For instance, if either $v_x > 200$ or $v_y > 200$, the hard threshold radar rescanning made it possible to additionally "catch" 103 single targets and 15 pairs of two targets for $m_\Delta < 5$. Meanwhile, although it is just 100 single targets additionally "caught" by the soft threshold radar rescanning, there are 23 pairs of two targets detected by the soft threshold (see the scatter in Fig. 4). Both threshold approaches have performed identically for either $v_x > 200$ or $v_y > 200$ and $m_\Delta < 1$: it is just 27 fast-moving single targets detected after rescanning, whereas none of pairs of two targets has been detected.

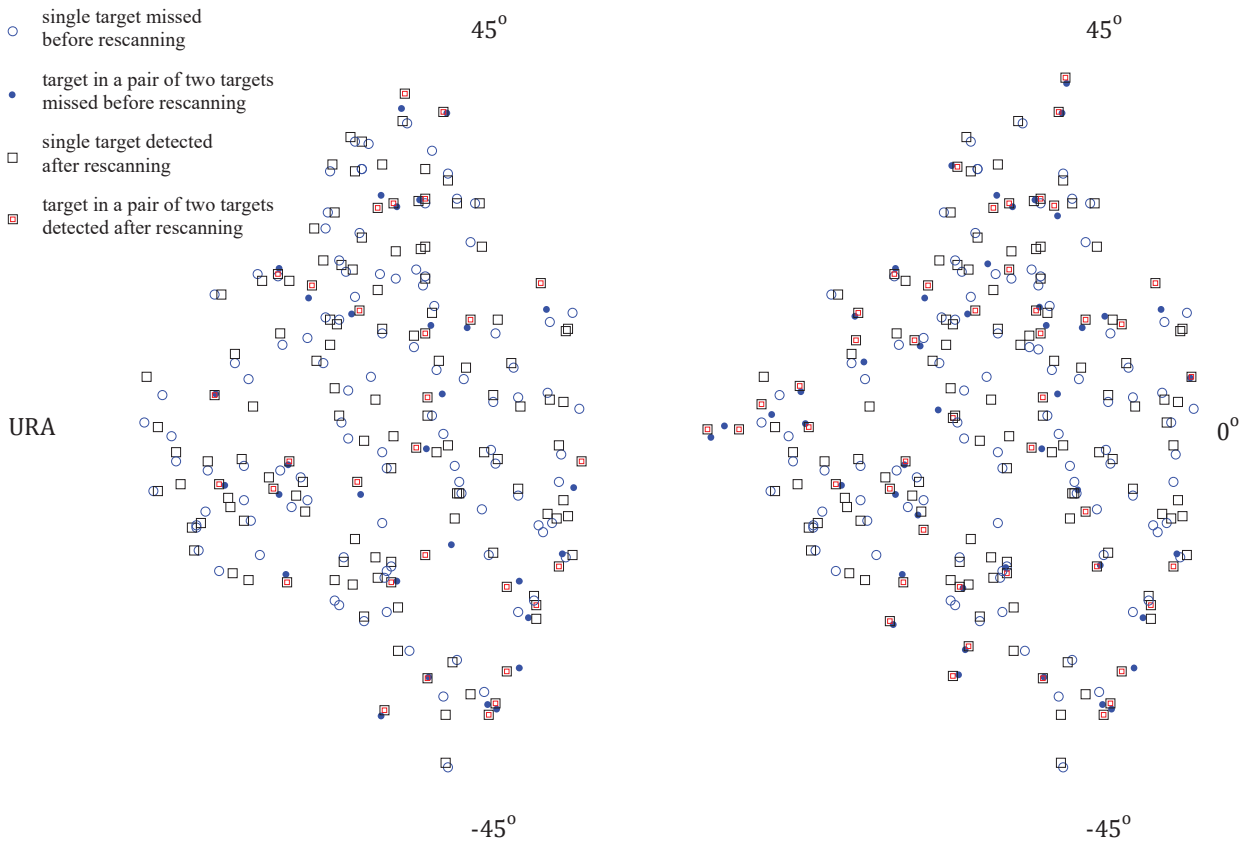

Fig. 4. Targets additionally "caught" by the hard threshold radar (left) and soft threshold radar (right) for $m_\Delta < 5$

As the rescanning precedes changing the URA size, it results in a decrement of URA sensors used to detect a target. This is confirmed by Table 3, where the lesser URA size on average is highlighted bold.

Table 3. Threshold and rescanning decrease the URA size

$m_\Delta < a_{est}$	Hard threshold				Soft threshold			
	Rescanning?				Rescanning?			
	no		yes		no		yes	
	average h	average w	average h	average w	average h	average w	average h	average w
$m_\Delta < 1$	**23.4**	**27.26**	23.42	27.3	**23.07**	**27.04**	**23.2**	**27.14**
$m_\Delta < 1.5$	**23.47**	**27.32**	23.57	27.4	**22.94**	**26.96**	**23.15**	**27.12**
$m_\Delta < 2$	22.48	26.66	**22.32**	**26.57**	**22**	**26.34**	**22.06**	**26.39**
$m_\Delta < 3$	22.15	26.43	**22.02**	**26.36**	**21.66**	**26.13**	**21.79**	**26.22**
$m_\Delta < 4$	22.14	26.43	**22.07**	**26.4**	**21.51**	**26.06**	**21.81**	**26.23**
$m_\Delta < 5$	22.11	26.41	**22.07**	**26.4**	**21.47**	**26.03**	**21.78**	**26.22**
$m_\Delta < 7$	22.12	26.42	**22.05**	**26.39**	**21.51**	**26.06**	**21.76**	**26.21**
$m_\Delta < 10$	22.13	26.43	**22.06**	**26.39**	**21.57**	**26.1**	**21.77**	**26.21**
$m_\Delta < 15$	22.12	26.42	**22.07**	**26.4**	**21.56**	**26.1**	**21.76**	**26.2**
$m_\Delta < 20$	22.13	26.42	**22.07**	**26.4**	**21.57**	**26.1**	**21.76**	**26.2**
$m_\Delta < 25$	22.12	26.42	**22.07**	**26.4**	**21.56**	**26.1**	**21.75**	**26.2**
$m_\Delta < 50$	22.13	26.42	**22.08**	**26.41**	**21.54**	**26.08**	**21.73**	**26.18**

9. Discussion

One must remember that the case when the rescanning is switched off implies a lower frequency of the ("regular") rescanning. When the rescanning is switched on, it means that its frequency is much higher. So, the rescanning, meant hereinabove to be switched on, requires some additional energy resource, unlike switching to the soft thresholding. The soft thresholding, when is factually fulfilled, takes some additional amount of time, but this amount is negligible.

Table 1 confirms that the soft threshold approach does not have a significant impact on the detection accuracy. The rescanning cannot increase the detection accuracy as well. However, when either the soft threshold or rescanning is applied, or they both are applied, the number of detections is increased (see Figs 3 and 4). The increment can be evaluated in approximately 2.7 %, whereas there have been 95.78 % detections by when the soft threshold and rescanning have been switched off against 98.42 % detections made by when the soft threshold and rescanning have been switched on (and applied when the hard threshold made a fail, and then possibly followed by a fail by the soft threshold).

When the soft threshold or rescanning is applied, or they both are applied, the expected high-accurate detection performance slightly drops. This is caused by that the soft thresholding and rescanning attempt at retrieving at least some information about the target instead of the detection fail (i. e., missing the target). It is the main limitation of the suggested soft threshold and rescanning — the accurate estimation of target parameters means more targets are detected, where the parameters of every "additionally" detected target are estimated with approximately the same accuracy (on average) as it is for the radar without soft thresholding and rescanning. Nevertheless, missing sufficiently less targets versus non-improved target parameter estimation is a strong tradeoff.

Some single targets and pairs of two targets (whose numbers are small, though) are detected with huge inaccuracies of the estimated parameters. Obviously, the detection accuracy cannot be estimated in real-world practice [1], [4], [11], [23], [33], [34]. Therefore, if even the target is factually missed due to huge inaccuracy in one or more of its parameters (about which a real-world observer does not know), the detection is anyway useful because it at least informs about a presence within the observed area. Later on, the target will probably be detected as the area is periodically rescanned (the low-frequency "regular" rescanning is meant) and the probability of the detection increases as the target remains with the area.

10. Conclusion

Based on simulating single-target and two-target detections by the URA-size-optimized radar, it is ascertained that using the threshold soft update approach along with a more frequent rescanning decreases a number of detection fails. Detecting two targets simultaneously moving through the radar area is a more difficult task compared to the single-target detection, but it nonetheless is improved by the soft thresholding and rescanning. Besides, the soft thresholding and rescanning allow slightly decreasing the number of URA sensors sufficient to maintain the same detection accuracy by increasing the averaged number of single-target and two-target detections at least by 2.5 %. The increment in a number of detected targets on average is equivalent to increasing the probability of detection. At almost the same accuracy of estimated parameters of the target, this is an improvement of the detection efficiency and accuracy.

Whether the suggested improvement will appear in the case of simultaneously moving three targets, without significantly dropping the averaged accuracy of estimation, is to be studied yet. It is clear that, as the number of simultaneous targets increases, the accuracy of a URA radar may significantly deteriorate due to just missing a single target in a group (e. g., a pair or triple) implies a detection fail.

References

1. M. K. Rad and S. M. H. Andargoli, "Power control and beamforming in passive phased array radars for low probability of interception," *Digital Signal Processing*, vol. 117, 103165, 2021.
https://doi.org/10.1016/j.dsp.2021.103165
2. Q. Cheng, S. Zheng, Q. Zhang, J. Ji, H. Yu, and X. Zhang, "An integrated optical beamforming network for two-dimensional phased array radar," *Optics Communications*, vol. 489, 126809, 2021.
https://doi.org/10.1016/j.optcom.2021.126809
3. L. Borowska, G. Zhang, and D. S. Zrnic, "Spectral processing for step scanning phased-array radars," *IEEE Transactions on Geoscience and Remote Sensing*, vol. 54, no. 8, pp. 4534 — 4543, 2016.
https://doi.org/10.1109/TGRS.2016.2543724
4. M. Skolnik, *Introduction to Radar Systems*, 3rd ed. New York City, New York, USA: McGraw-Hill, 2001.
5. H. J. Visser, *Array and Phased Array Antenna Basics*, Hoboken, New Jersey, USA: John Wiley & Sons, 2006.
https://doi.org/10.1002/0470871199
6. R. Sturdivant, C. Quan, and E. Chang, *Systems Engineering of Phased Arrays*, Norwood, Massachusetts, USA: Artech House, 2018.
7. H. Asplund et al., "Chapter 4 — Antenna Arrays and Classical Beamforming," in *Advanced Antenna Systems for 5G Network Deployments: Bridging the Gap Between Theory and Practice*, P. von Butovitsch, Ed. Cambridge, Massachusetts, USA: Academic Press, 2020, pp. 89 — 132.
https://doi.org/10.1016/B978-0-12-820046-9.00004-6
8. V. V. Romanuke, "Minimal total weighted tardiness in tight-tardy single machine preemptive idling-free scheduling," *Applied Computer Systems*, vol. 24, no. 2, pp. 150 — 160, 2019.
https://doi.org/10.2478/acss-2019-0019
9. V. V. Romanuke, "Decision making criteria hybridization for finding optimal decisions' subset regarding changes of the decision function," *Journal of Uncertain Systems*, vol. 12, no. 4, pp. 279 — 291, 2018.
10. R. Gui, Z. Zheng, and W.-Q. Wang, "Cognitive FDA radar transmit power allocation for target tracking in spectrally dense scenario," *Signal Processing*, vol. 183, 108006, 2021.
https://doi.org/10.1016/j.sigpro.2021.108006
11. P. Fritsche and B. Wagner, "Evaluation of a novel radar based scanning method," *Journal of Sensors*, vol. 2016, Article ID 6952075, 2016.
https://doi.org/10.1155/2016/6952075
12. W. E. Kock, *Radar, Sonar, and Holography: An Introduction*, Cambridge, Massachusetts, USA: Academic Press, 1973.

https://doi.org/10.1016/C2013-0-10981-6
13. H. Meikle, *Modern Radar Systems*, 2nd ed. Artech House Publishers, 2008.
14. V. V. Romanuke, "Uniform rectangular array radar optimization for efficient and accurate estimation of target parameters," *Information and Telecommunication Sciences*, vol. 13, no. 1, pp. 44 — 55, 2022.
15. Z. Li and X. Zhang, "Monostatic MIMO radar with nested L-shaped array: Configuration design, DOF and DOA estimation," *Digital Signal Processing*, vol. 108, 102883, 2021.
https://doi.org/10.1016/j.dsp.2020.102883
16. H. Gao, M. Chen, Y. Du, and A. Jakobsson, "Monostatic MIMO radar direction finding in impulse noise," *Digital Signal Processing*, vol. 117, 103198, 2021. https://doi.org/10.1016/j.dsp.2021.103198
17. M. O. Kolawole, "5 — The radar equations," in *Radar Systems, Peak Detection and Tracking*, Elsevier, 2002, pp. 105 — 155.
https://doi.org/10.1016/B978-075065773-0/50008-X
18. L. Zhang, Y. Wang, Y. Hou, and J. Song, "Uniform rectangular distribution of far-field intensity by optical phased array," *Optics Communications*, vol. 507, 127661, 2022.
https://doi.org/10.1016/j.optcom.2021.127661
19. H. S. Dawood, H. A. El-Khobby, M. M. Abd Elnaby, and A. H. Hussein, "A new optimized quadrant pyramid antenna array structure for back lobe minimization of uniform planar antenna arrays," *Alexandria Engineering Journal*, vol. 61, iss. 8, pp. 5903 — 5917, 2022.
https://doi.org/10.1016/j.aej.2021.11.018
20. W. Xing, H. Zhang, H. Chen, Y. Yang, and D. Yuan, "Feature adaptation-based multipeak-redetection spatial-aware correlation filter for object tracking," *Neurocomputing*, vol. 488, pp. 299 — 314, 2022.
https://doi.org/10.1016/j.neucom.2022.02.072
21. R. N. Simon, T. Tormos, and P.-A. Danis, "Very high spatial resolution optical and radar imagery in tracking water level fluctuations of a small inland reservoir," *International Journal of Applied Earth Observation and Geoinformation*, vol. 38, pp. 36 — 39, 2015.
https://doi.org/10.1016/j.jag.2014.12.007
22. L. M. Novak, G. J. Owirka, and C. M. Netishen, "Radar target identification using spatial matched filters," *Pattern Recognition*, vol. 27, iss. 4, pp. 607 — 617, 1994. https://doi.org/10.1016/0031-3203(94)90040-X
23. C. Wang, B. Jiu, and H. Liu, "Maneuvering target detection in random pulse repetition interval radar via resampling-keystone transform," *Signal Processing*, vol. 181, 107899, 2021.
https://doi.org/10.1016/j.sigpro.2020.107899
24. Y.-Y. Dong, C.-X. Dong, W. Liu, and M.-M. Liu, "DOA estimation with known waveforms in the presence of unknown time delays and Doppler shifts," *Signal Processing*, vol. 166, 107232, 2020.
https://doi.org/10.1016/j.sigpro.2019.07.025
25. N. H. Nguyen and K. Doğançay, "Single-platform passive emitter localization with bearing and Doppler-shift measurements using pseudolinear estimation techniques," *Signal Processing*, vol. 125, pp. 336 — 348, 2016.
https://doi.org/10.1016/j.sigpro.2016.01.023
26. W. Huang and R. Lin, "Efficient design of Doppler sensitive long discrete-phase periodic sequence sets for automotive radars," in *2020 IEEE 11th Sensor Array and Multichannel Signal Processing Workshop (SAM)*, Hangzhou, China, 2020, pp. 1 — 5.
https://doi.org/10.1109/SAM48682.2020.9104358
27. R. Amiri and A. Shahzadi, "Micro-Doppler based target classification in ground surveillance radar systems," *Digital Signal Processing*, vol. 101, 102702, 2020.
https://doi.org/10.1016/j.dsp.2020.102702
28. P. Zhang and X. Zhang, "Multiple missiles fixed-time cooperative guidance without measuring radial velocity for maneuvering targets interception," *ISA Transactions*, Available online 17 July 2021.
https://doi.org/10.1016/j.isatra.2021.07.023
29. T. Lyu, C. Li, Y. Guo, and G. Ma, "Three-dimensional finite-time cooperative guidance for multiple missiles without radial velocity measurements," *Chinese Journal of Aeronautics*, vol. 32, iss. 5, pp. 1294 — 1304, 2019.
https://doi.org/10.1016/j.cja.2018.12.005
30. B. Yan, A. Giorgetti, and E. Paolini, "A track-before-detect algorithm for UWB radar sensor networks," *Signal Processing*, vol. 189, 108257, 2021.
https://doi.org/10.1016/j.sigpro.2021.108257
31. G. Shan, G. Xu, and C. Qiao, "A non-myopic scheduling method of radar sensors for maneuvering target tracking and radiation control," *Defence Technology*, vol. 16, iss. 1, pp. 242 — 250, 2020.
https://doi.org/10.1016/j.dt.2019.10.001
32. T. Jian, J. Liu, S. Zhou, and W. Liu, "Target detection with persymmetric subspace models for steering vector mismatches in MIMO radars," *Digital Signal Processing*, vol. 126, 103480, 2022.
https://doi.org/10.1016/j.dsp.2022.103480
33. L. Hongbo, S. Yiying, and L. Yongtan, "Estimation of detection threshold in multiple ship target situations with HF ground wave radar," *Journal of Systems Engineering and Electronics*, vol. 18, iss. 4, pp. 739 — 744, 2007.
https://doi.org/10.1016/S1004-4132(08)60013-4
34. H. Sun, M. Li, L. Zuo, and R. Cao, "Joint threshold optimization and power allocation of cognitive radar network for target tracking in clutter," *Signal Processing*, vol. 172, 107566, 2020.
https://doi.org/10.1016/j.sigpro.2020.107566

Романюк В.В.

Коректне виявлення декількох об'єктів радаром на основі рівномірно-прямокутної фазованої антенної решітки з м'яким оновленням порогу та повторним скануванням області

Проблематика. Якщо інтенсивність рухомих об'єктів у межах спостережуваної області є низькою, оптимальною кількістю сенсорів рівномірно-прямокутної фазованої антенної решітки (РПФАР) радара є або в РПФАР мінімального розміру (або близького до нього), або в РПФАР максимального розміру (або близького до нього), де розмір РПФАР регулюється за допомогою (симетричного) вимкнення вертикальних та горизонтальних сенсорів. Однак це не гарантує виявлення будь-якого об'єкта, оскільки іноді порогове виявлення, за яким оцінюються основні параметри одного об'єкта або пари об'єктів, не спрацьовує навіть за підходу з м'яким порогом, коли поріг поступово зменшується під час зривів виявлення.

Мета дослідження. Для покращення виявлення декількох наземних об'єктів РПФАР-радаром необхідно зменшити кількість зривів виявлення, коли об'єкти просто втрачаються. Для цього використовуються підхід з м'яким оновленням порогу та множина квазіоптимальних розмірів РПФАР, включаючи РПФАР розмірів 20×25 і 35×35, з повторним скануванням області у випадку зриву виявлення.

Методика реалізації. Для досягнення мети проводиться симуляція РПФАР-радара на множині випадково генерованих об'єктів, де приблизно половина елементів цієї множини складається з одного об'єкта, а інша половина — з пар об'єктів. Симуляція та її конфігурування відбуваються за допомогою функцій MATLAB® R2021b Phased Array System Toolbox™ на основі моделі моностатичного радара.

Результати дослідження. Ані підхід м'якого порогу, ані повторне сканування не збільшують точність виявлення. Однак коли застосовується м'який поріг або повторне сканування, або обидва підходи одночасно, це збільшує кількість виявлень. Таке збільшення може бути оцінено приблизно у 2.7 %, але очікувана продуктивність високоточних виявлень дещо спадає. Це викликано тим, що м'який поріг та повторне сканування намагаються дістати принаймні якусь інформацію про об'єкт замість того, щоб його втратити.

Висновки. Використання підходу м'якого оновлення порогу разом з більш частішим скануванням зменшує кількість зривів виявлення. Крім того, м'який поріг та повторне сканування дозволяють дещо зменшити кількість сенсорів РПФАР, достатню для підтримки того ж рівня точності виявлення при збільшенні середньої кількості однооб'єктних та двооб'єктних виявлень щонайменше на 2.5 %. Зростання кількості виявлених об'єктів у середньому еквівалентно збільшенню імовірності виявлення.

Ключові слова: *радар на основі фазованої антенної решітки; рівномірно-прямокутна антенна решітка; спостережувана область; об'єкт; поріг виявлення; повторне сканування.*